

Performance Prediction of Bundle Double-Walled Carbon Nanotube-Composite Materials for Dipole Antennas at Terahertz Frequency Range

Yaseen N. Jurn^{1,*}, Sawsen A. Mahmood², and Imad Q. Habeeb¹

Abstract—In this paper, the double-walled carbon nanotube composite material (DWCNTs-composite) and bundle of DWCNT-composite material (CB-DWCNTs) for antenna applications at terahertz frequency range are presented and investigated. The mathematical modeling and analysis of DWCNTs-composite material is presented for the purpose of modelling and simulation approach. The bundle of DWCNTs-composite material is constructed and designed, based on this modeling approach. The DWCNT-composite material consists of double-walled carbon nanotube coated by a thin jacket of another different material. The dependency of the electrical conductivity of B-DWCNTs-composite on different parameters is presented and investigated. The performance evaluation of B-DWCNTs-composite and CB-DWCNTs materials are presented based on their electromagnetic properties. For this purpose, the dipole antennas of these composite materials are designed and implemented using CST (MWS), where the cross sections of B-DWCNTs-composite and CB-DWCNT materials are circular geometry. Furthermore, comparative studies are performed to show the dependency of size and frequency of the DWCNT-composite material. The results obtained from the DWCNTs-composite and CB-DWCNTs dipole antennas are presented based on S_{11} parameters, resonant frequency, gain, bandwidth, and efficiency.

1. INTRODUCTION

In modern antenna technology, CNTs antennas are at the forefront of research, due to their unique electrical properties [1–4]. Based on the results of these works, poor efficiency and high input impedance are the main problems of CNTs-dipole antennas. Therefore, in our previous research, we proposed using CNTs-composite material instead of CNTs material without changing CNTs original structure, in order to enhance the electromagnetic (EM) performance of the CNTs dipole antennas [5–8]. A great deal of our research and other research were proposed using bundle of SWCNTs (B-SWCNTs), in order to overcome problems related to SWCNTs-dipole antennas [9–15]. In these works, the dipole antennas of B-SWCNTs were designed and implemented using different universal techniques, in order to estimate the EM properties of B-SWCNTs. Also, the purpose of B-SWCNTs is to mitigate the input impedance problem of the individual SWCNT, as well as to improve the radiation efficiency of CNTs dipole antenna.

On the other hand, CNTs materials are mixed with different materials to produce several types of CNTs composite materials for antenna and other applications. These composite materials have been used to designed and implemented different antenna types for several applications [16–21].

Recently, progress on the controlled growth of DWCNTs has been presented and discussed for different applications [22]. Terahertz electrical properties and optical characteristics of DWCNTs were

Received 16 October 2019, Accepted 20 December 2019, Scheduled 16 January 2020

* Corresponding author: Yaseen Naser Jurn (yaseen.naser@uoitc.edu.iq).

¹ Department of Mobile Communications and Computing Engineering, Engineering Collage, University of Information Technology and Communications, Baghdad, Iraq. ² Department of Computer Science, Collage of Education, Al-Mustanseria University, Iraq.

presented in previous work and compared with SWCNT structure [23]. However, there has been no report so far about utilizing the DWCNTs coated by copper, silver, and graphite in antenna applications. In this work, the DWCNTs which consist of two concentric single-walled carbon nanotubes are utilized to construct a new composite material structure (DWCNTs-composite).

In this paper, a new CNTs antenna structure is proposed to operate efficiently in THz frequency band. The proposed antenna is composed of a bundle of DWCNTs-composite material structure, where each DWCNT is surrounded by another material jacket. The outer jacket is a thin layer of graphite or copper material. Mathematical modelling approach is presented for this structure for the purpose of modeling and simulation for antenna applications. The efficiency, gain, S_{11} parameter, resonant frequency, and bandwidth of B-DWCNT-composite material dipole antennas are presented. The simulation results show that these parameters are considerably enhanced at the THz frequencies relative to the B-DWCNTs bundle antenna.

2. METHODOLOGY

In this work, the DWCNTs-composite is adopted to construct the bundle of DWCNTs composite material (B-DWCNTs-composite). Likewise, the DWCNTs-composite material is presented based on coating the DWCNTs by a jacket of another material, such as graphite and copper. The B-DWCNTs-composite is presented to produce new material structures, which are necessary for designing dipole antennas for the future technology.

This paper is presented to study, analyze, design, and estimate the EM properties of B-DWCNTs-composite dipole antennas at THz frequency band, based on new DWCNTs-composite materials. The progress of this work is presented as follows: First, present the structure of the new DWCNT-composite material. Second, explain the configuration of B-DWCNTs-composite material. Third, the main mathematical modeling and analysis of these structures are presented and explained.

2.1. Structure of DWCNTs-Composite Material

The new material is presented in this work, which consists of DWCNT coated by a thin jacket of graphite material to construct (DWCNT-graphite) and copper to construct (DWCNT-copper) material structures. The structure of DWCNTs-composite material is illustrated in Figure 1. In this figure, the innermost radius of DWCNTs-composite structure is denoted by r_1 , and the outermost radius is denoted by r_2 , while the average thickness of jacket is denoted by t , and R is the total radius of DWCNTs-composite tube ($R = r_2 + t$) with length of tube denoted by (L_S). This work assumes $L_1 = L_2$, which means that the terminals at the two ends of composite tube have the same dimensions and dependent on the dimensions of DWCNT. The electrical conductivity of new DWCNT-composite material structure consists of four parts, in which Part1 & Part2 represent the jacket material at the two ends of composite tube; Part3 represents the jacket material over the DWCNT; and Part4 represents the DWCNT material.

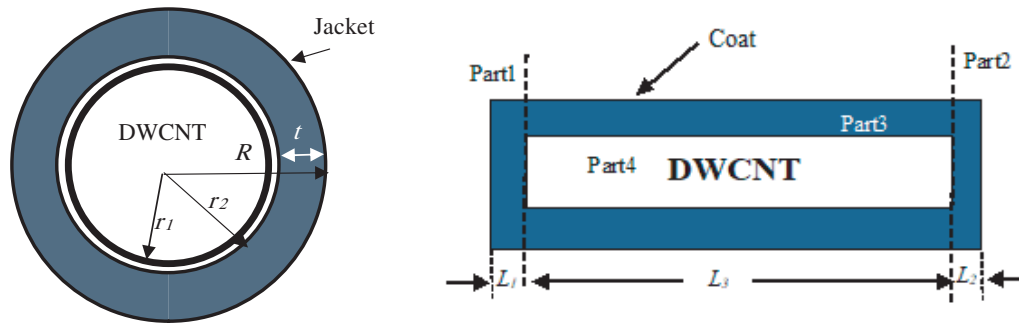


Figure 1. The schematic of DWCNTs-composite material structure.

2.2. Configuration of Bundles

In this work, the B-DWCNTs-composite structure contains (N) number of metallic double-walled carbon nanotubes composite material tubes which are identical. These tubes have the same dimensions and coated by a thin jacket of another material. The bundle B-DWCNTs-composite has configuration characterized by a closely packed structure with a circular geometrical structure. The B-DWCNTs-composite tubes are aligned parallel along the axis of bundle, and the lattice constant of the bundle is (Δ) to personify the distance between each two contiguous tubes of DWCNTs-composite tubes. The minimum required radius of the bundle that contains all DWCNTs-composite is (R_B). Figure 2 explains the sketch of a B-DWCNTs-composite structure with a circular geometrical structure.

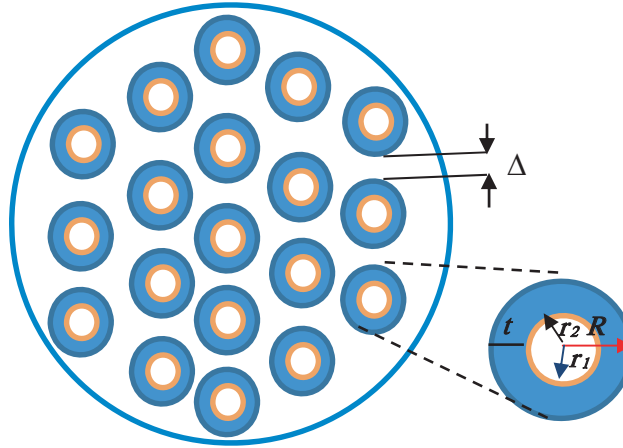


Figure 2. Schematic configuration of B-DWCNTs-composite material structure.

2.3. Mathematical Modeling and Analysis of DWCNTs-Composite Structure

In this section, the mathematical modeling and analysis of B-DWCNTs-composite structure is presented and explained for the purpose of modeling and investigation of this composite structure. The influences of the DWCNT dimensions and average thickness layer of jacket material are related significantly with the electrical conductivity of the DWCNT-composite structure. The estimation of the electrical conductivity for this composite structure is applied for modeling and EM simulation into the CST (MWS). In this mathematical modeling approach, the electrical conductivity of the new composite structure is denoted by (σ_{DWC}). Meanwhile, the conductivity of jacket layer is denoted by (σ_{jacket}). The mathematical model of the DWCNTs-composite is derived based on the mixture rule, for a simple parallel model of the radial interface of coating material and DWCNT.

Therefore, the electrical conductivity of this composite structure has been derived to obtain the general formula of this electrical conductivity presented as follows:

$$A_{DWC}\sigma_{DWC} = C_{DWCNT}L_3\sigma_{DWCNT} + A_{jacket}L_3\sigma_{jacket} + 2A_{tip}L_2\sigma_{jacket} \quad (1)$$

where (A_{DWC}) represents the cross-sectional area of DWCNTs-composite structure, (C_{DWCNT}) the cross-section area of DWCNT (circumference of DWCNT), (A_{jacket}) the radial cross-sectional area of jacket material, and (σ_{DWCNT}) the electrical conductivity of DWCNT presented in previous research [2, 23–25]. Then, the final expression of this conductivity is presented as follows:

$$\pi R^2\sigma_{DWC}(w) = (2\pi R^2L_2 + \pi(R^2 - r_2^2)L_3)\sigma_{jacket} + 2\pi r_2L_3 \left(\frac{2}{r_2} \sum_{n=1}^2 r_n\sigma_{DWCNT,n} \right) \quad (2)$$

$$\sigma_{DWC}(w) = \frac{1}{R^2} \left[(2R^2L_2 + (R^2 - r_2^2)L_3)\sigma_{jacket} + 4L_3 \sum_{n=1}^2 r_n\sigma_{DWCNT,n} \right] \quad (3)$$

$$\sigma_{DWC}(w) = \frac{1}{R^2} \left[(2R^2L_2 + (R^2 - r_2^2)L_3)\sigma_{jacket} + 4L_3 \left(r_1 \frac{-j2e^2V_f}{\pi^2hr_1(w - jv)} + r_2 \frac{-j2e^2V_f}{\pi^2hr_2(w - jv)} \right) \right] \quad (4)$$

$$\sigma_{DWC}(w) = \frac{1}{R^2} \left\{ (2R^2L_2 + (R^2 - r_2^2)L_3)\sigma_{jacket} + 32L_3 \left[\frac{e^2V_f v}{\pi^2h(w^2 + v^2)} - j \frac{e^2V_f w}{\pi^2h(w^2 + v^2)} \right] \right\} \quad (5)$$

where r_n is the radius of the relevant DWCNT, n the wall numbers of DWCNT, e the electron charge, h the reduced Plank's constant ($h = 1.05457266 \times 10^{-34} J.s$), t the average thickness of jacket, V_f the Fermi velocity of CNT ($V_f = 9.71 \times 10^5$ m/s), and v the estimated phenomenological relaxation frequency ($v = 6T/r$) [24], when T is the temperature in kelvin, so $F_v = v/2\pi$, and w is the angular frequency.

For the purpose of EM modeling and simulation, the plasma frequency (W_{DWC}) is an important parameter of the DWCNT-composite material that must be computed in this mathematical modeling approach.

$$W_{DWC} = \frac{e}{\pi R} \left[\frac{32V_f + \pi^2hD}{h\varepsilon^o} \right]^{1/2} \quad (6)$$

where

$$D = \left(\frac{(R^2 - r^2)v\sigma_{jacket}}{e^2} \right) \quad (7)$$

The relative complex permittivity of the DWCNTs-composite is derived based on the material parameters reported in this mathematical modeling approach and the general mathematical relation between the complex permittivity and plasma frequency.

$$\varepsilon'_{DWC} = 1 - \frac{w_{DWC}^2}{w^2 + v^2} \quad (8)$$

where,

$$\varepsilon''_{DWC} = \frac{v w_{DWC}^2}{w^3 + wv^2} \quad (9)$$

ε'_{DWC} and ε''_{DWC} represent the real and imaginary parts of the relative complex permittivity of the DWCNTs-composite. From the above mathematical representation and analysis for the DWCNTs-composite, one can conclude that the electrical conductivity, relative complex permittivity, and plasma frequency are affected by several parameters such as the conductivity of jacket material (σ_{jacket}) and average thickness of jacket material (t). In another context, the EM behavior of this composite structure will be changed corresponding to the changing of these parameters.

2.4. Simulation Modeling of B-DWCNTs Composite

For the purpose of simulation modeling of B-DWCNTs and B-DWCNTs-composite in the CST (MWS), the important parameters of DWCNT-composite are extracted in this work. Likewise, the important parameters of DWCNT applied in this work are extracted depending on the previous works [22]. Hence, these parameters are employed to represent the DWCNT and DWCNT-composite by equivalent bulk material into CST (MWS). The main objective of this modeling approach is to enable simple and efficient EM analysis for the B-DWCNT and B-DWCNTs-composite through the CST (MWS). After inserting the important parameters of DWCNT and DWCNT-composite structures into the CST (MWS) Drude dispersion model, the B-DWCNT and B-DWCNTs-composite can be designed to extract the EM properties of the circular B-DWCNT and B-DWCNTs-composite, based on the design of the dipole antennas for these bundles.

In this work, to design and investigate the B-DWCNT and B-DWCNT-composite dipole antennas, the DWCNT and DWCNT-composite tube are connected and aligned in parallel in these bundles, in order to form the dipole antennas structures. The structure of B-DWCNT and B-DWCNTs-composite dipole antenna includes two packed bundles of the DWCNT and DWCNT-composite, respectively, separated by a small feeding gap.

Also, each packed bundle is connected to a square contact, in order to make a feeding source connected to all DWCNT-composites. The dimensions of this contact (length \times width) are ($W_D \times T_D$),

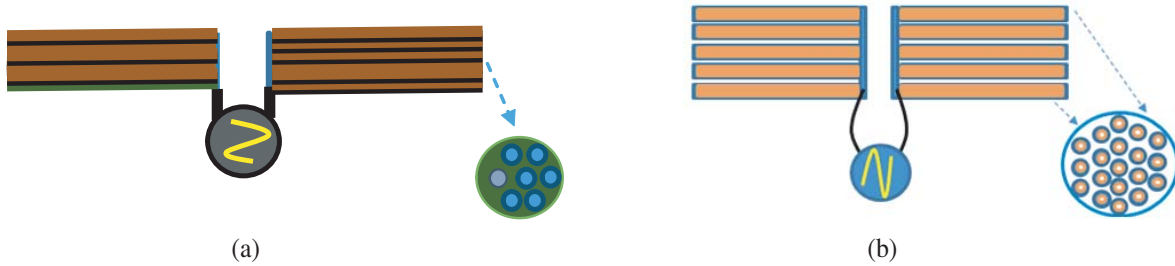


Figure 3. Schematic dipole antenna structures for both (a) B-DWCNTs and (b) B-DWCNTs-composite.

while the thickness is equal to the outer radius of the DWCNT-composite (R) for DWCNT-composite dipole antenna and equal to the outermost radius of DWCNT (r_2) for the DWCNT dipole antenna. Hence, the length and width of this contact are similar and equal to the diameter of bundles $2R_B$. The diagrams of dipole antennas structures for both B-DWCNT and B-DWCNTs-composite are illustrated in Figure 3.

3. SIMULATION RESULTS

In order to estimate the EM properties of B-DWCNTs and B-DWCNTs-composite materials, their dipole antennas are designed and implemented using CST (MWS). In this work, the lattice distance between DWCNT-composite contiguous tubes is approximately 0.34 nm, and the DWCNT consists of armchair (metallic) walls. The validity of the tube wall conductivity and scattering model for the single wall case have been discussed in [15, 22–25]. The length of these dipole antennas is ($L = 20 \mu\text{m}$); innermost radius of DWCNT is ($r_1 = 2.71 \text{ nm}$); the outermost radius of DWCNT is ($r_2 = 3.062 \text{ nm}$); the length of jacket material at two terminals of the tube is $L_1 = L_3 = 0.010L_2$; the average thickness of jacket material is ($t = 2 \text{ nm}$). Four values of the number of tubes DWCNTs ($N = 7, 19, 37$ and 61) are mainly used in those simulation results, in order to investigate the comparison among B-DWCNTs, B-DWCNTs-graphite, and B-DWCNT-copper dipole antennas.

In order to predict the behavior of the electrical conductivity of B-DWCNTs-composite materials, several simulations are carried out. These simulations are utilized to explain the behavior dependency of these structures on different parameters. In these simulation results, the behaviours of the electrical conductivity of DWCNTs-composite materials are presented to explain the conductivity scaling with length of DWCNT, outermost radius of DWCNTs, average thickness of jacket layer, and radius of DWCNTs-composite tube. In this work, the length of coating material at two terminals of the tube is $L_1 = L_3 = 0.010L_2$. Figure 4 presents the effects of the tube length on the electrical conductivity of DWCNTs-composite. The dependency of conductivity of DWCNTs-composite structure on the outmost radius of DWCNT is illustrated in Figure 5. Figure 6 illustrates the dependency of conductivity of DWCNTs-composite structure on the average thickness of jacket layer. The effect of DWCNTs-composite radius on the electrical conductivity of these composite structures is illustrated in Figure 7.

As illustrated in these results, the conductivity is directly proportional to the radius of DWCNT-composite structure and outmost radius of DWCNT, based on Figure 5 and Figure 7, respectively. The conductivity is directly proportional to the length of DWCNT-composite structure as illustrated in Figure 4 and the average thickness of jacket layer as illustrated in Figure 6. The electrical conductivity of the DWCNTs-composite structure will be better with larger length, outmost radius of DWCNT, radius of DWCNTs-composite structure, and average thickness of jacket layer.

The EM simulation results of the B-DWCNTs and B-DWCNTs-composite dipole antennas are presented in this work, based on fixed dipole antenna lengths $L = 20 \mu\text{m}$ and different numbers of DWCNTs-composite tubes in the bundle structure such as ($N = 7, 19, 37$ and 61). The main material parameters of DWCNTs and DWCNTs-composite structure are mathematically derived and inserted into the CST (MWS), Drude dispersion model as a new normal material into CST(MWS). These parameters are plasma frequency, relative complex permittivity, and phenomenological relaxation. This

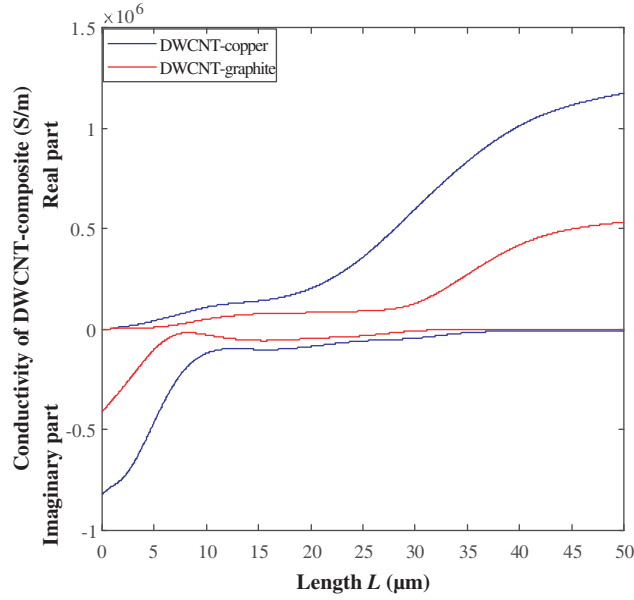


Figure 4. Effects of the tube length on the DWCNTs-composite conductivity.

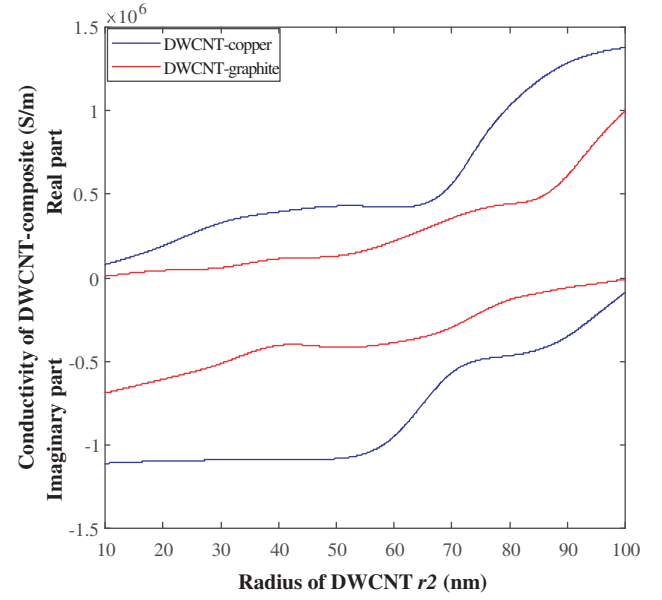


Figure 5. Effects of the outmost radius of DWCNT on the conductivity of DWCNTs-composite.

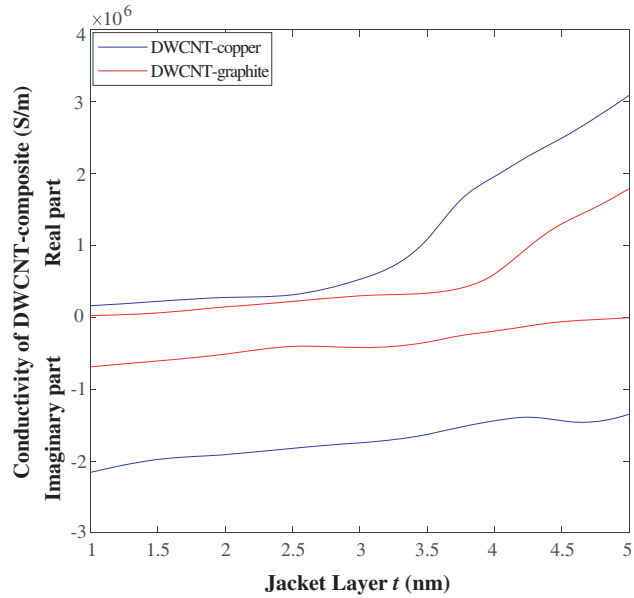


Figure 6. Dependency of DWCNTs-composite conductivity on the average thickness of jacket layer.

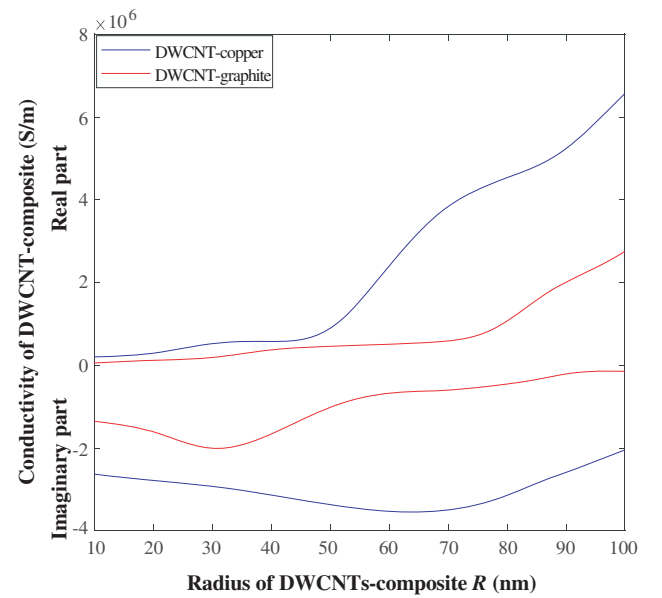


Figure 7. The effects of DWCNTs-composite tube radius on the conductivity of this structure.

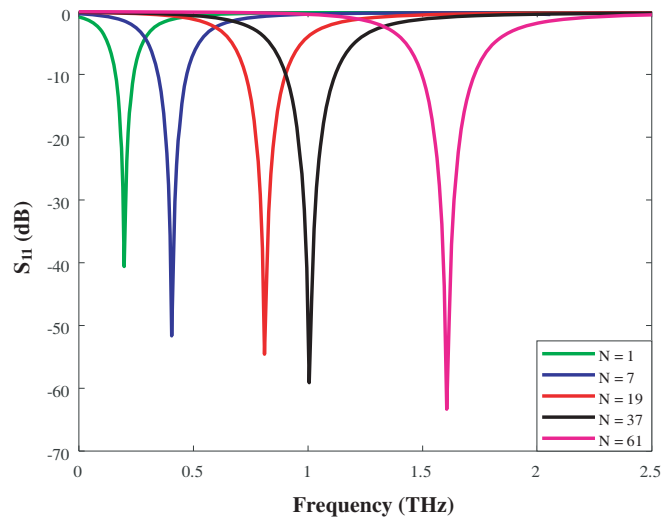
approach makes the representation of these structures into CST (MWS) available. The dipole antenna of both B-DWCNTs-composite and B-DWCNTs structures are designed and implemented, in order to estimate their EM properties.

In this work, simulation results of S_{11} parameter of B-DWCNTs are illustrated in Figure 8, whereas the simulation results of S_{11} parameter of B-DWCNTs-graphite and B-DWCNT-copper dipole antennas are displayed in Figure 9 and Figure 10, respectively.

On the bases of the simulation results for both B-DWCNTs and B-DWCNTs-composite dipole

Table 1. Summary of comparison results for B-DWCNTs, B-DWCNTs-composite structures.

Total number of tubes in the bundles (N)	B-DWCNTs No coating		B-DWCNTs-graphite After coated by graphite material		B-DWCNTs-copper After coated by copper material	
	Resonant Frequency (THz)	S_{11} parameter (dB)	Resonant Frequency (THz)	S_{11} parameter (dB)	Resonant Frequency (THz)	S_{11} parameter (dB)
1	0.25	-40	0.13	-45.4	1.0	-45.10
7	0.42	-51.6	0.24	-56.1	1.23	-51.00
19	0.73	-55.4	0.46	-60.20	1.60	-54.80
37	1.0	-60.5	0.63	-66.20	2.0	-61.10
61	1.64	-65.3	1.1	-70.10	2.60	-64.70

**Figure 8.** Simulation results of B-DWCNTs dipole antenna at length ($L = 20 \mu\text{m}$) and ($N = 1, 7, 19, 37$, and 61).

antennas, Table 1 presents the summary of comparisons for the simulation results of these structures.

From the presented results in Figures 8–10 and Table 1, the behaviours of S_{11} parameters of B-DWCNTs-composite have been enhanced compared with B-DWCNTs. It means that S_{11} parameter is changed after coating the DWCNT by a thin jacket of copper and graphite materials. The coating of DWCNTs by a thin jacket of graphite material leads to shifting-down the resonant frequency of dipole antenna compared with resonant frequency of B-DWCNT dipole antenna. On the contrary, the coating of DWCNT by a thin jacket of copper material leads to shifting-up the resonant frequency of its dipole antenna compared with resonant frequency of B-DWCNT dipole antenna. Therefore, the B-DWCNTs-copper dipole antenna could be used for high frequency applications; meanwhile, the B-DWCNTs-graphite dipole antenna could be used for lower frequency applications compared with B-DWCNTs dipole antenna.

Finally, in order to compare the antenna efficiency among B-DWCNTs, B-DWCNTs-graphite, and B-DWCNTs-copper dipole antennas, scientific simulations are implemented. These simulations have been implemented based on antenna length ($L = 20 \mu\text{m}$), inner radius of DWCNT ($r_1 = 2.71 \text{ nm}$), outmost radius of DWCNT ($r_2 = 3.062 \text{ nm}$), average thickness of coating layer ($t = 2 \text{ nm}$), and the

number of tubes (DWCNT, DWCNTs-graphite and DWCNTs-copper) in the bundles is ($N = 7$). The simulation results of these comparisons are illustrated in Figure 11. From these results, the efficiencies of both B-DWCNTs-copper and B-DWCNTs-graphite dipole antennas are higher than B-DWCNTs dipole antenna. Also, the B-DWCNTs-graphite dipole antenna has a good efficiency at low frequency band and the B-DWCNTs-copper dipole antenna at high frequency band.

4. DISCUSSION

In order to predict the EM performance of B-DWCNTs, B-DWCNTs-graphite, and B-DWCNTs-copper material structures, their dipole antennas have been designed and implemented using CST (MWS). The simulation results of these dipole antennas are illustrated in Figures 8–10. The reported results of this work display S_{11} parameters to explain the behavior of different DWCNTs structures with respect to frequency variations and different numbers of tubes in the bundles. From the results, the resonant frequency of these bundles shifts up by increasing the number of tubes in the bundle. The coated DWCNT by graphite material leads to decreasing the resonant frequency (shifting down) compared

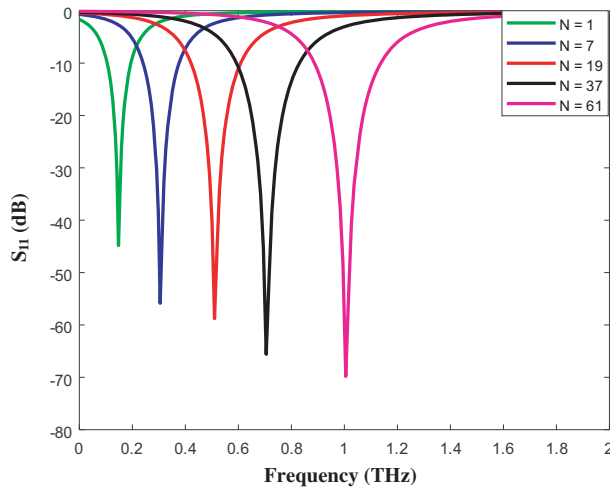


Figure 9. Simulation results of B-DWCNTs-graphite dipole antenna at length ($L = 20 \mu\text{m}$) and ($N = 1, 7, 19, 37$ and 61).

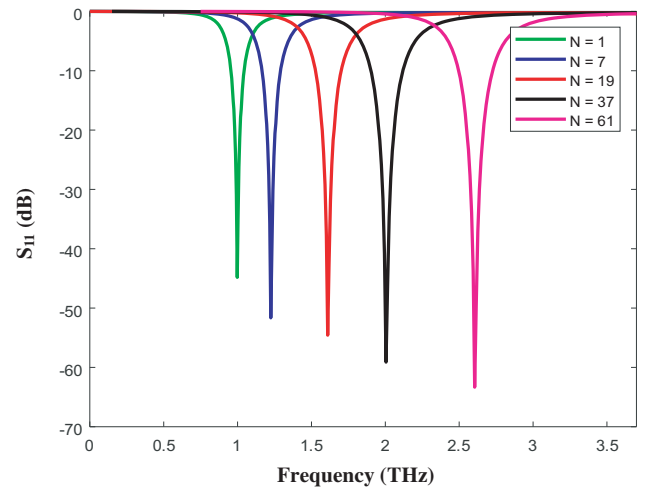
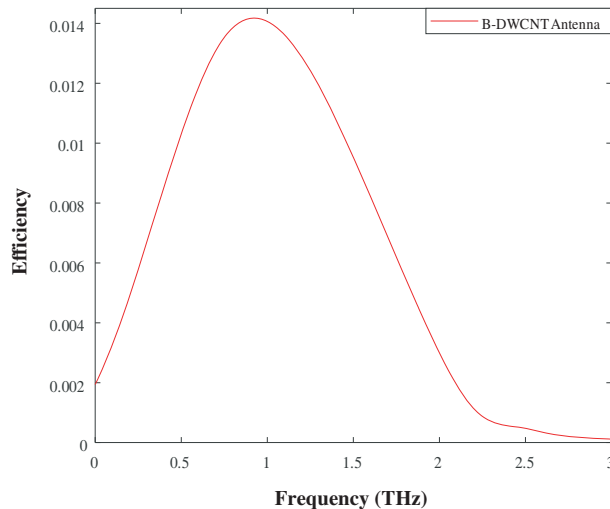
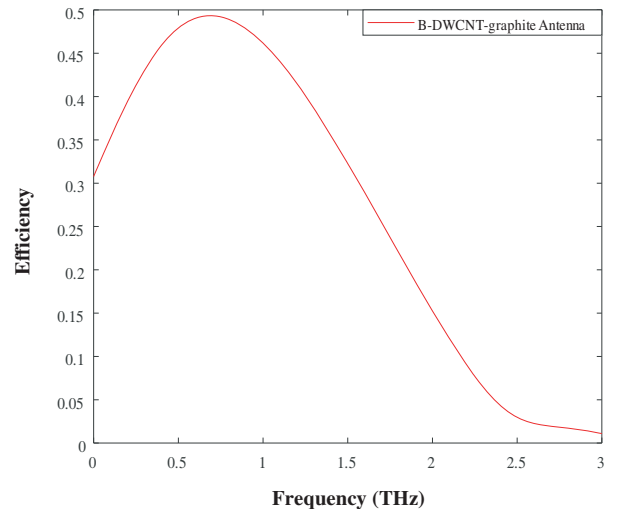


Figure 10. Simulation results of B-DWCNTs-copper dipole antenna at length ($L = 30 \mu\text{m}$) and ($N = 1, 7, 19, 37$ and 61).



(a)



(b)

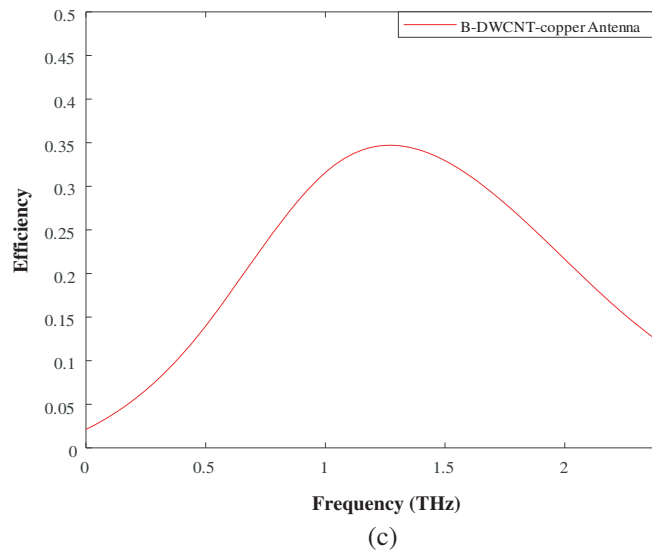


Figure 11. Efficiency of (a) B-DWCNTs dipole antenna, (b) B-DWCNTs-graphite dipole antenna and (c) B-DWCNTs-copper dipole antenna, at dipole antenna length $L = 20 \mu\text{m}$ and $N = 7$.

with the simulation results of B-DWCNTs dipole antenna. Likewise, by comparing the simulation results of B-DWCNTs and B-DWCNTs-copper dipole antennas, the coated DWCNT by a thin layer of copper material leads to (shifting up) the resonant frequency of B-DWCNTs-copper dipole antenna.

From Figure 11, the efficiency of B-DWCNTs dipole antenna is improved after coated the DWCNT by graphite and copper materials, due to changing the material properties of DWCNTs and influences of graphite and copper materials.

5. CONCLUSIONS

In this paper, the performance evaluation of the two bundles B-DWCNTs-graphite and B-DWCNTs-copper have been investigated to present these structures as new materials for designing new dipole antennas. These dipole antennas could be used for different applications instead of the dipole antennas of original structures of CNTs. On the bases of the simulation results presented in this paper, the coated DWCNT by a thin layer jacket of graphite material leads to decreasing the resonant frequency, while the coated DWCNT by a thin jacket layer of copper leads to increasing the resonant frequency. In addition, the efficiencies of dipole antennas of these new structures have been enhanced after coating the DWCNT by graphite and copper materials. These material structures are represented as new material structures for different antenna applications at terahertz frequency band.

REFERENCES

1. Burke, P., C. Rutherglen, and Z. Yu, "Carbon nanotube antennas," *Proceedings of Joint 9th International Conference on Electromagnetics in Advanced Applications*, 937–940, Torino, Italy, 2005.
2. Hanson, G. W., "Fundamental transmitting properties of carbon nanotube antennas," *IEEE Transactions on Antennas and Propagation*, Vol. 53, No. 11, 3426–3435, 2005.
3. Journ, Y. N., M. F. Malek, and W.-W. Liu, "Investigation of single-wall carbon nanotubes at THz antenna," *ICED Conference*, 415–420, Malaysia, 2014.
4. Journ, Y. N., M. F. Malek, and W.-W. Liu, "Investigation of single-wall carbon nanotubes at THz antenna," *Malaysia International Conference on Communications (MICC)*, 246–251, Malaysia, 2015.

5. Jurn, Y. N., M. F. Malek, and W.-W. Liu, "A 60 GHz single-walled carbon nanotube composite material for dipole antenna applications," *Malaysia International Conference on Communications (MICC)*, 323–328, Malaysia, 2015.
6. Jurn, Y. N., M. F. B. A. Malek, and H. A. Rahim, "Mathematical analysis and modeling of single-walled carbon nanotube composite material for antenna applications," *Progress In Electromagnetics Research M*, Vol. 45, 59–71, 2016.
7. Jurn, Y. N., M. F. Abdul Malek, and H. A. Rahim, "Carbon nanotubes composite materials for dipole antennas at terahertz range," *Progress In Electromagnetics Research M*, Vol. 66, 11–18, 2018.
8. Jurn, Y. N., M. F. Malek, and W.-W. Liu, "Important parameters analysis of the single-walled carbon nanotubes composite materials," *ARPJ Journal of Engineering and Applied Sciences*, Vol. 11, No. 8, 5108–5113, 2016.
9. Jurn, Y. N., M. F. Malek, and W.-W. Liu, "An investigation of single-walled carbon nanotubes bundle dipole antenna at THz frequencies," *IEEE International Conference on Control System, Computing and Engineering*, 565–570, 2014.
10. Jurn, Y. N., M. F. Malek, and Sawsen A. Mahmood, "Performance evaluation of the electromagnetic behavior of the bundle SWCNTs with circular geometry," *CONECCT Conference*, 1–6, India, 2015.
11. Jurn, Y. N., M. F. Malek, and Sawsen A. Mahmood, "Modelling and simulation of rectangular bundle of single-walled carbon nanotubes for antenna applications," *Journal of Key Engineering Materials*, Vol. 701, 57–66, 2016.
12. Jurn, Y. N., M. F. Malek, and Sawsen A. Mahmood, "Electromagnetic modelling of bundle of single-walled carbon nanotubes with circular geometry for antenna applications," *ACES Journal*, Vol. 32, No. 6, 531–541, 2017.
13. Huang, Y., W. Y. Yin, and Q. H. Liu, "Performance prediction of carbon nanotube bundle dipole antennas," *IEEE Transactions on Nanotechnology*, Vol. 7, No. 3, 331–337, 2008.
14. Choi, S. and K. Sarabandi, "Performance assessment of bundled carbon nanotube for antenna applications at terahertz frequencies and higher," *IEEE Transactions on Antennas and Propagation*, Vol. 59, No. 3, 802–809, 2011.
15. Hanson, G. W. and J. Hao, "Infrared and optical properties of carbon nanotube dipole antennas," *IEEE Transactions on Nanotechnology*, Vol. 5, No. 6, 766–775, 2006.
16. Mehdipour, A., I. D. Rosca, A. R. Sebak, W. Christophe, and S. V. Hoa, "Full-Composite fractal antenna using carbon nanotubes for multiband wireless applications," *IEEE Antennas and Wireless Propagation*, Vol. 9, 891–894, 2010.
17. Mehdipour, A., I. D. Rosca, A. R. Sebak, W. Christophe, and S. V. Hoa, "Carbon nanotube composites for wideband millimeter-wave antenna applications," *IEEE Transactions on Antennas and Propagation*, Vol. 59, No. 10, 3572–3578, 2011.
18. Aissa, B., M. Nedil, M. Habib, and D. Therriault, "Fluidic patch antenna based on liquid metal alloy/single-wall carbon-nanotube operating at the S-band frequency," *Applied Physics Letters*, Vol. 103, No. 5, 063101-1–063101-5, 2013.
19. Alvarez, N. T., T. Ochmann, N. Kienzle, B. Ruff, M. R. Haase, T. Hopkins, S. Pixley, D. Mast, M. J. Schulz, and V. Shanov, "Polymer coating of carbon nanotube fibers for electric microcables," *Nanomaterials*, Vol. 4, 879–893, 2014.
20. Hanium Marmia, K. and T. Mieno, "Production and properties of carbon nanotube/cellulose composite paper," *Journal of Nanomaterials*, Article ID 6745029, pages 11, 2017.
21. Amram Bengio, E., D. Senic, L. W. Taylor, R. J. Headrick, M. King, P. Chen, C. A. Little, J. Ladbury, C. J. Long, C. L. Holloway, A. Babakhani, J. C. Booth, N. D. Orloff, and M. Pasquali, "Carbon nanotube thin film patch antennas for wireless communications," *Appl. Phys. Lett.*, Vol. 114, 203102-1–203102-5, 2019.
22. Fujisawa, K., H. J. Kim, H. Muramatsu, T. Hayashi, T. C. Hirschmann, M. S. Dresselhaus, Y. A. Kim, and P. T. Araujo, "A review of double-walled and triple-walled carbon nanotube synthesis and applications," *Appl. Sci.*, Vol. 6, No. 109, 1–32, 2016.

23. Maeng, I., C. Kang, S. J. Oh, and J.-H. Sonb, "Terahertz electrical and optical characteristics of double-walled carbon nanotubes and their comparison with single-walled carbon nanotubes," *Applied Physics Letters*, Vol. 90, 051914 (1-3), 2007.
24. Hanson, G. W. and J. A. Berres, "Multiwall carbon nanotubes at RF-THz frequencies: Scattering, shielding, effective conductivity, and power dissipation," *IEEE Transactions on Antennas and Propagation*, Vol. 59, No. 8, 3098–3103, 2011.
25. Jurn, Y. N., M. F. Malek, and H. A. Rahim, "Performance assessment of the simulation modeling approach of SWCNT at THz and GHz antenna applications," *IEEE 12th Malaysia International Conference on Communications (MICC)*, 246–251, 2015.